Study of Imidazole-Based Proton-Conducting Composite Materials Using Solid-State NMR

S. R. Benhabbour,[†] R. P. Chapman,[†] G. Scharfenberger,[‡] W. H. Meyer,[‡] and G. R. Goward*,[†]

McMaster University, Hamilton, Ontario, Canada, and Max Planck Institute for Polymer Research, Mainz, Germany

Received September 28, 2004. Revised Manuscript Received December 17, 2004

The application of solid-state NMR methods to characterize the structure and dynamics of imidazole-based proton-conducting polymeric materials provides insight into the mechanism (Grotthus vs vehicle) of proton-mobility. The presented materials are built on a siloxane backbone, and are of interest as potential new proton-conducting membranes for fuel cells able to function at temperatures above 130 °C. This is expected to improve the CO tolerance of the catalyst in the fuel cell, as compared to water-based systems. High-resolution solid-state ^{1}H NMR is achieved under fast magic-angle spinning (MAS) conditions (30 kHz), and provides resolution of resonances in the hydrogen-bonding region. Homonuclear double quantum filtered (DQF) NMR spectra, acquired using the back-to-back sequence, provided identification of mobile protons. It was found that proton conductivity, observed macroscopically using impedance spectroscopy, is correlated with local proton mobility, observed via ^{1}H NMR line width trends observed for the hydrogen-bonded protons. ^{1}H MAS and DQF NMR experiments show no crystal packing of these materials in contrast to model oligo-ethyleneoxide-tethered imidazole materials (Imi-*n*EO) studied previously. Comparisons of macroscopic and microscopic measures of proton mobility are also presented in the activation energies of pure and acid-doped siloxane oligomers and polymers functionalized with imidazole. The acid-doped materials show enhanced proton mobility, and hence higher conductivity, relative to the pure material.

Introduction

Research in the field of proton conductivity in the past few years has been driven by the goal of developing suitable proton-conducting materials for application in all solid-state electrochemical devices, such as batteries, smart windows, sensors, and most importantly, fuel cells.[1−3] Common polymer-electrolyte membrane fuel cells (PEMFCs) use hydrated ionomers, such as NAFION, as membrane electrolytes. Although Nafion proved remarkable conductivities of 10^{-3} to 10^{-2} Ω^{-1} cm^{-1} at room temperature, in addition to excellent mechanical properties, these materials rely on the presence of water for proton conduction and exhibit a noticeable drop in conductivity at temperatures above the water dew point.[1] Moreover, Nafion suffers other disadvantages such as high cost, poor hydrophilicity, and fuel crossover.[4] With the aim of developing PEMFCs operating at temperatures above 130 °C in low humidity environments, a new class of polymer electrolytes has been investigated.[5]

Previously, it has been reported that substituting water as a proton solvent by heterocycles, such as imidazole, benzimidazole, or pyrazole in ionomers results in competitive conductivity at much higher temperatures than those viable in hydrated systems, as high as 200 °C.[6] Model compounds consisting of short oligo-ethyleneoxide (EO) chains terminated by an imidazole group (Imi-*n*EO),[7] are used for comparison with the new composite materials in this study. The proton conductivity of the Imi-*n*EO materials has been studied previously by solid-state NMR.[8] In these model systems the EO segments used as spacers for the imidazole groups tethered to the polymer backbone were varied in length to study the influence of chain length on the local dynamics of the terminating imidazole groups, as well as proton mobility. In these systems proton transport involves the diffusion of a structural defect in a hydrogen bond network, also known as the Grotthus mechanism, in contrast to hydrated polymer systems, in which proton transport occurs via the molecular diffusion of protons with water, known as vehicle transport.[6] The key distinction between the two mechanisms is the ability or necessity of the vehicle molecules, H_2O in this case, to travel with the ion being transported in the former model, whereas the ion mobility is independent of long-range mobility of a vehicle in the Grotthus mechanism, also termed structural diffusion. The

* Corresponding author. Tel: (905)525-9140, ext 24176. E-mail: goward@mcmaster.ca.
† McMaster University.
‡ Max Planck Institute for Polymer Research.

(1) Roziere, J.; Jones, D. *Annu. Rev. Mater. Res.* **2003**, *33*, 503−555.
(2) Schuster, M.; Meyer, W. *Annu. Rev. Mater. Res.* **2003**, *33*, 233−261.
(3) De Zea Bermudez, V.; Poinsignon, C.; Armand, M. B. *J. Mater. Chem.* **1997**, *7* (9), 1677−1692.
(4) Mauritz, K. A.; Moore, R. B. *Chem. Rev.* **2004**, *104*, 4535−4586.
(5) Herz, H. G.; Kreuer, K. D.; Maier, J.; Scharfenberger, G.; Schuster, M.; Meyer, W. H. *Electrochem. Acta* **2003**, *48*, 2165−2171.
(6) Kreuer, K. D.; Fuchs, A.; Ise, M.; Spaeth, M.; Maier, J. *Electrochem. Acta* **1998**, *43*, 1281−1288.
(7) Schuster, M.; Meyer, W. H.; Wegner, G.; Herz, H. G.; Ise, M.; Schuster, M.; Kreuer, K. D.; Maier, J. *Solid State Ionics* **2001**, *145*, 85−92.
(8) Goward, G. R.; Schuster, M.; Sebastiani, D.; Schnell, I.; Spiess, H. W. *J. Phys. Chem. B.* **2002**, *106*, 9322−9334.

10.1021/cm048301l CCC: $30.25
Published on Web 02/22/2005

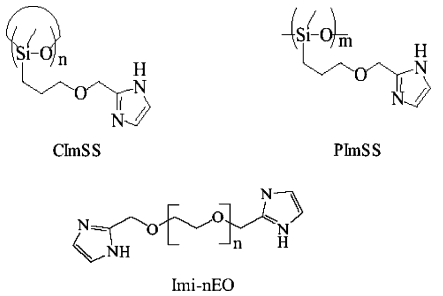

Figure 1. Chemical structure of the materials: cyclic siloxane oligomers (CImSS), linear polysiloxanes (PImSS), and model compound Imi-*n*EO.

necessity for small molecule "vehicles" is the limiting factor governing the operating temperature of many current PEMFC membrane candidates.[5]

These model systems provided the basis for a more extended study, which targeted true polymeric materials, as well as hybrid inorganic/organic composites based on the imidazole system. The goal of such synthetic work was to move beyond small molecules toward a class of materials which could be processed as thin-films, as well as offering improved electrochemical stability. In work by Scharfenberger et al.[9] imidazole was again used as proton solvent, to enable fast proton transport within a hydrogen-bond network. Several imidazole-based polymer electrolytes were synthesized via two different approaches. Imidazole was covalently linked to a linear polysiloxane backbone (PImSS), or linked to a cyclic siloxane oligomer (CImSS), as illustrated in Figure 1. For such systems, proton conductivity must completely rely on structure diffusion and local segmental motion rather than the molecular self-diffusion of solvated protons. Polymeric siloxanes were selected to afford a high concentration of charge carriers located at the heterocyclic groups within the truly polymeric systems.[9] The pure CImSS, for example, shows a proton conductivity of about 10^{-4} S/cm.[9]

In the present study we investigate the above imidazole−siloxane systems in terms of their structural and dynamic properties using high-resolution solid-state NMR. The application of advanced solid-state NMR methods provides insight into the mechanism of proton-mobility in these novel materials. High-resolution solid-state ^{1}H NMR is achieved under fast MAS conditions (30 kHz), and provides resolution of resonances in the hydrogen-bonding region. Homonuclear double quantum NMR spectra, which selectively probe through-space (dipolar) couplings, provide information concerning the relative proton mobilities. ^{29}Si and ^{13}C NMR spectra confirm the local structure of the amorphous materials. Moreover, variable temperature ^{1}H MAS NMR measurements are compared to the proton conductivity measurements, to elucidate the mechanism of proton conductivity, as compared to the Imi-*n*EO model materials. These measurements also allow calculation of activation energies, which were found to be comparable to those obtained with the Imi-*n*EO model materials.

Previous studies on the Imi-*n*EO systems,[8] mentioned above, showed that hydrogen-bonded structures are formed between imidazole rings resulting in short-range ordered domains. This has been shown in the ^{1}H NMR spectra of the Imi-*n*EO samples studied, where a pair of resonances at high frequency was observed corresponding to the strongly H-bonded protons.[8] These protons have restricted mobility and hence do not participate in proton transport. In such systems, the proton conductivity is attributed to the disordered portions of the materials.

Here we investigate proton conductivity of imidazole-based polyelectrolytes (Figure 1) with the goal of finding possible structural and dynamic similarities with the model Imi-*n*EO systems, and providing a clearer picture of structural and conductivity relationship. As well, we have characterized materials doped with small percentages of triflic acid, which has been shown to dramatically enhance conductivity. It is proposed to provide protonic defects in the hydrogen-bonding network, thereby increasing the number of charge carriers in the system. In related work, we have demonstrated through exchange-based solid-state NMR studies that ring-reorientation in imidazolium methylsulfonate has an activation energy on the order of 60 kJ/mol in the salt,[10] and is thought to be the rate-limiting step for proton-transport in imidazole-based materials.

^{1}H NMR Methods

Solid-state NMR spectroscopy is a valuable tool for studying proton conductivity in polyelectrolyte systems. The ability to observe the specific nuclei of interest directly, due to the excellent NMR sensitivity and resolution provides a very useful tool to study the electronic environment of the protons and for probing the presence of hydrogen bonding specifically. Another very useful application of solid-state NMR techniques lies in the ability to directly measure the relative strength of ^{1}H−^{1}H dipolar interactions, which are directly related to the molecular mobility. In solid-state ^{1}H NMR, the high resolution is achieved by magic-angle spinning (MAS) at frequencies typically of 30 kHz.

The imidazole substituents can exhibit $\pi-\pi$ stacking and hydrogen bonding. Both phenomena can be specifically probed in the solid state, in contrast to solution state, where these effects are removed due to molecular tumbling and dilution. Additional information including ^{1}H−^{1}H dipole−dipole interactions can be provided using multidimensional NMR experiments. For instance, high resolution can be achieved by combining fast MAS with 2D multiple-quantum (MQ) spectroscopy, thus allowing the structural and dynamic information inherent to the dipolar couplings to be accessed.[11] Depending on how strong the ^{1}H−^{1}H dipolar couplings are, two alternative experimental methods can be used. Strong couplings generate dipolar DQ coherences between a pair of protons, the signals of which can be correlated with their individual resonances in a 2D DQF spectrum. Using rotor-synchronized homonuclear ^{1}H−^{1}H double-quantum filtered (DQF) MAS experiments, an example of which is the back-to-back (BABA) pulse sequence, differentiation between distinct H-bonding motifs can be achieved. Since these

(9) Scharfenberger, G. et al. Ph.D. Thesis, Johannes Gutenberg University Mainz, Germany, 2003. http://ArchiMeD.uni-mainz.de/pub/2003/0113.

(10) Goward, G. R.; Fischbach, I.; Saalwachter, K.; Spiess, H. W. *J. Phys. Chem. B.* **2004**, *108*, 18500−18508.

(11) Brown, S. P.; Spiess, H. W. *Chem. Rev.* **2001**, *101*, 4125−4155.

structural domains are the key in structural diffusion or transport of protons, this resolution is essential for the success of our approach. Moreover, by analyzing the presence of coherence or absence of a DQF coherence, for a given resonance observed in the standard 1D MAS experiment, we are able to distinguish between strongly and weakly coupled nuclei, corresponding to rigid and mobile molecules, respectively. Here, mobile molecules are those which are mobile on the time-scale of the DQF experiment, i.e., 1−2 rotor periods, or 25−50 μs. DQF experiments have been applied in the present study to investigate the rigid parts in the above systems. Weak couplings tend to generate incoherent processes, such as dipolar cross relaxation found in NOE (nuclear Overhauser effect) experiments, making NOE spectroscopy, or 2D NOESY, also known as 2D exchange spectroscopy (EXSY), the most appropriate approach to targeting the mobile protons directly.[8] The NOESY experiment does not rely on strong dipolar coupling, and thus allows us to probe local interactions between mobile parts of the molecules. Since this local mobility is critical to long-range proton transport, this is also a very valuable experiment, allowing for investigation of the local structure and its relation to ion transport. In the limit of fast MAS, NOESY spectra behave similarly to solution-state NOESY spectra.[12]

The mobility present in the materials can be investigated through variable-temperature ^{1}H MAS spectra, where comparative H-bonding strengths can be observed. In general, two cases can be encountered in an NMR experiment. In the first case, where the local motion in a system is fast on the NMR time scale, information on fast proton transfer is reflected through the proton line widths, which is related to the spin−spin relaxation times (T_2*).[13] On the other hand, if the local motions within a system are slow with respect to the NMR time scale, they can be detected via chemical shift trends of the resonances involved in slow exchange, a phenomenon also known as coalescence.[5] These processes have been used in the present study and are discussed in more detail in the results section.

Experimental Section

Sample Preparation. The materials were synthesized as described in ref 6 and handled such that exposure to moisture was excluded.

Solid-State NMR. ^{1}H MAS NMR experiments were performed on a Bruker DRX 500 spectrometer using a double-resonance MAS probe supporting rotors of 2.5-mm outer diameter with a spinning frequency of up to 30 kHz. The Larmor frequency of ^{1}H is 500.13 MHz. The spectra are referenced to adamantane (1.63 ppm, ^{1}H). ^{1}H NMR spectra were acquired using a 90° pulse length of 2.0 μs, a recycle delay of 2 s, and with the bearing gas at room temperature. DQ MAS experiments were performed with one cycle of the BABA recoupling sequence.[15] The rotor-synchronized 2D ^{1}H−^{1}H DQ spectra were recorded using a full back-to-back sequence, with $\tau_{exc} = \tau_R$ with t_1 increments set equal to one rotor period.[14] 2D NOESY exchange spectra were acquired using mixing times between 0.01 and 20 ms. This pulse sequence was applied in a rotor-synchronized fashion, with increments of the indirect dimension time constant, t_1, of one rotor period, or 25 μs, and mixing times of n rotor periods.

^{13}C CP-MAS spectra were acquired on a Bruker DRX 300 spectrometer operating at a ^{13}C Larmor frequency of 75.44 MHz, under 8 kHz MAS, with contact times of 5 ms. The spectra are referenced to glycine (176 ppm, ^{13}C). ^{29}Si CP-MAS spectra were acquired on a Bruker DRX 300 spectrometer operating at a ^{29}Si Larmor frequency of 59.60 MHz, under 2 kHz MAS, with contact times of 5 ms.

Temperature Calibrations under Fast MAS. It is well-known that fast magic-angle spinning induces a significant amount of frictional heating within the rotor.[15] It is possible to calibrate this frictional heating using a chemical shift thermometer such as $Sm_2Sn_2O_7$.[16] This was done by first synthesizing the samarium stannate using sol−gel chemistry and hydrothermal synthesis. The purity of the product was confirmed by powder X-ray diffraction. An NMR sample was prepared by mixing a small amount of SnO_2 with the $Sm_2Sn_2O_7$. Subsequently, variable-temperature ^{119}Sn NMR spectra were acquired under various spinning speeds, and the chemical shift difference between the isotropic peaks from the two tin environments were measured as a function of both temperature and spinning speed. The data were analyzed according to the relationships reported in the literature,[17] and the resulting calibration was applied to determine the sample temperatures (T_s) for given bearing gas temperatures (T_b) and spinning speeds (ν_r). This temperature correction, established for our 2.5-mm probe, was applied to all the variable-temperature studies reported here.

Results and Discussion

Identifying Mobile Protons: ^{1}H MAS and 1D DQF NMR. Here we describe a number of experimental results which, when combined, provide a clear insight on the microscopic processes related to proton transport in the compounds presented in Figure 1. For comparison, the ^{1}H MAS and homonuclear DQF spectra of Imi-2EO, CImSS, and PImSS systems are shown in Figure 2. In all cases, the spectra show strong broad aliphatic and aromatic signals, as well as smaller, but more telling N−H resonances at high frequency. In contrast to model Imi-*n*EO systems, no complex crystal packing was observed for the CImSS and PImSS systems. This is evidenced by the number of N−H resonances in the ^{1}H MAS spectra, where only one N−H resonance is observed in both CImSS and PImSS systems at frequencies of 12 and 14.5 ppm, respectively. In the model Imi-2EO system, however, three different N−H resonances were obtained in the ^{1}H MAS NMR spectra. Such multiple high-frequency resonances are expected for molecules that form multiple hydrogen-bonding networks in the solid state. The comparison of the MAS (upper) and DQF (lower) spectra shows that the N−H resonances as well as the aromatic protons on the imidazole ring in both CImSS and PImSS systems are eliminated or diminished by the DQ-filtration experiment. Therefore, the resonances at the aromatic region and at higher frequency corresponding to

(12) Bain, A. D. *Prog. Nucl. Magn. Reson. Spectrosc.* **2003**, *43*, 63−103.
(13) (a) Becker, E. D. *High-Resolution NMR Theory and Chemical Applications*, 3rd ed.; Academic Press: San Diego, CA, 2000; pp 30−32. (b) Harris, R. K. *Nuclear Magnetic Resonance Spectroscopy: A Physiochemical View;* Pitman Books Ltd.: London, 1983; p 122.
(14) Schnell, I.; Spiess, H. W. *J. Magn. Reson.* **2001**, *151*, 153−227.
(15) Grimmer, A.-R.; Kretschmer, A.; Cajipe, V. B. *Magn. Reson. Chem.* **1997** *35*, 86.
(16) van Moorsel, G.-J.; van Eck, E. R.; Grey, C. P. *J. Magn. Reson.* **1995**, *113*, 159.
(17) Langer, B.; Schnell, I.; Spiess, H. W.; Grimmer, A.-R. *J. Magn. Reson.* **1999**, *138*, 182.

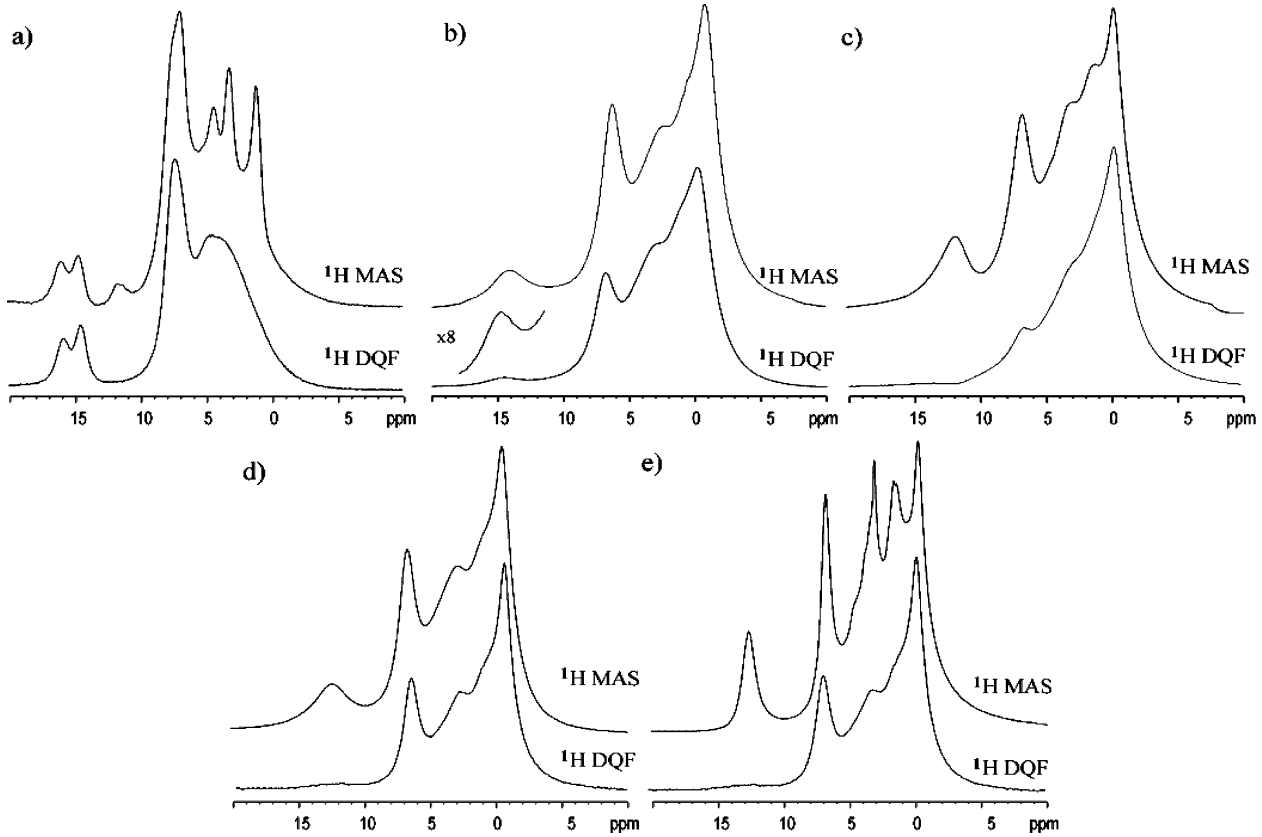

Figure 2. Comparison of ^{1}H MAS (top) spectra with double quantum filtered spectra (bottom) for (a) Imi-2EO, (b)PImSS, (c) CImSS, (d) PImSS + 10% triflic acid, and (e) CImSS + 10% triflic acid.

the protons on the imidazole ring are attributed to the "mobile" protons, whose dipolar interactions are significantly reduced by the molecular motion. The behavior of the N−H resonance is consistent with its participation in proton transport. Additionally, the reduced intensity of aromatic resonances indicates that they experience local motion, causing the averaging of their strong intramolecular dipolar interactions. Mobility is proposed to occur as ring-reorientation about the tethered apex of the imidazole ring. These data support the hypothesis of ring-reorientation acting as the rate-limiting step in conductivity. This rate-limiting step has been investigated in the related salt material, imidazolium methylsulfonate, using advanced solid-state NMR methods,[21] and also studied extensively in imidazole itself by means of ab initio molecular dynamics simulations.[18]

H-Bonding and Local Contacts: 2D ^{1}H DQF and NOESY Spectra. The strongly hydrogen-bonded molecules can be selectively investigated using ^{1}H−^{1}H 2D DQ NMR spectroscopy, since DQ coherences are generated only from relatively strong ^{1}H−^{1}H dipole−dipole couplings, in other words, from protons in very close proximity to each other.[3] Such a 2D DQF spectrum is shown in Figure 3 for PImSS.

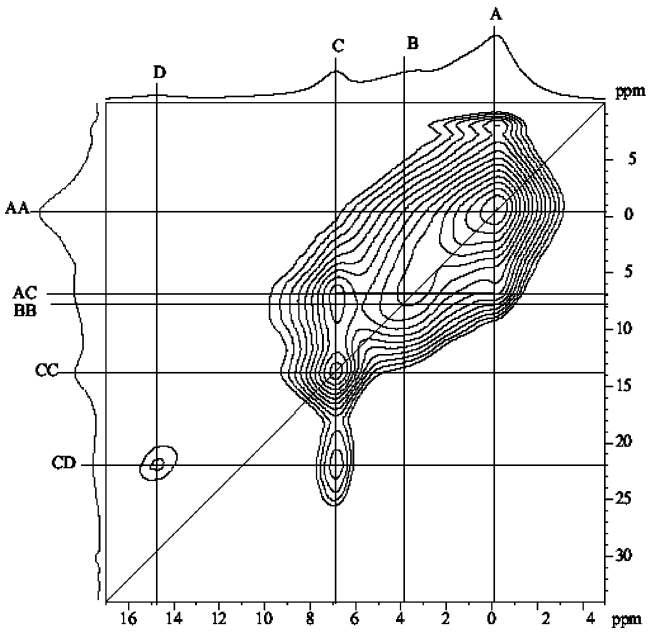

Figure 3. 2D ^{1}H DQF spectrum of PImSS acquired at 25 kHz MAS, under ambient bearing gas temperature, with one rotor period of recoupling.

The dominant feature in the above 2D spectrum arises along the diagonal, representing the dipolar couplings between the "like" protons in the siloxane-bound methyl groups (**AA**), the ethylene oxide CH_2 groups (**BB**), and aromatic regions (**CC**). As well, the correlation between these protons is observed as a pair of off-diagonal resonances at **AC**. There is a shoulder on the left of the CH_2 resonance, which is attributable to the different types of CH_2 environments: those

(18) Munch, W.; Kreuer, K. D.; Silvestri, W.; Maier, J.; Seifert, G. *Solid State Ionics* **2001**, *145*, 437−443.
(19) Colomban, Ph., Ed. *Proton Conductors: Solids, Membranes, and Gels − Materials and Devices*; Cambridge University Press: Cambridge, 1992.
(20) Temperature calibrations were performed using a $Sm_2Sn_2O_7$ chemical shift thermometer, according to the methods described by Langer et al..
(21) Goward, G. R.; Fischbach, I.; Saalwachter, K.; Spiess, H. W. *Solid State NMR* **2003**, *24*, 150−162.

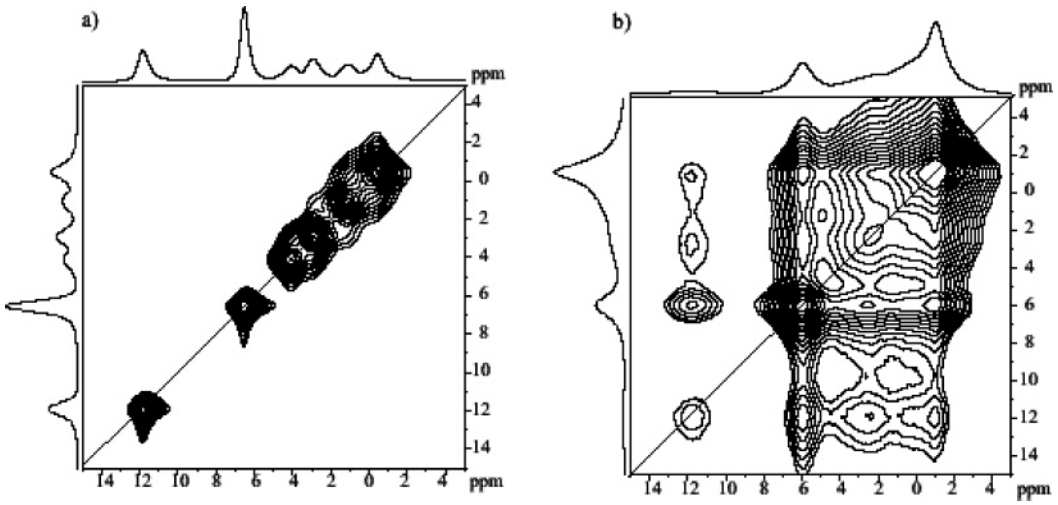

Figure 4. ^{1}H NOESY spectra of PImSS doped with 10% triflic acid, acquired under ambient bearing gas temperature, at 25 kHz MAS with (a) $t_{mix} = 20$ μs and (b) $t_{mix} = 2$ ms.

next to the oxygen, and those next to other CH_2 or silicon centers. Although the resolution is not adequate to make an exact assignment, this is a logical interpretation of the broadening. The lower left corner is the most informative region of the spectrum, illustrating the hydrogen bonds formed within the system. The observed weak correlation between the aromatic resonance and the N−H resonance at **CD** illustrates the comparative weakness of this dipolar coupling, consistent with the 1D observations. This confirms that these protons have a greater degree of mobility than the rest of the molecule. However, it is interesting to note that a comparable spectrum of Imi-2EO shows no resonance for this mobile N−H, while strong correlations for the rigid domains of the material, which have stronger H-bonding, are observed.[8] The absence of peaks along the diagonal at the N−H resonance, **DD**, indicates that the hydrogen-bonding NH protons are not close in space to each other; therefore, only intramolecular contact is observed. The other feature in this spectrum is the absence of the off-diagonal peak, **AD**, corresponding to the interaction between the aliphatic protons of the EO linking chain and the aromatic protons on the imidazole ring. This result excludes any short contact between the N−H and the ethylene sidechain, or siloxane backbone, thus giving evidence for clustering of the imidazole rings, and excluding a more disordered or tangled conformation at this temperature, or among the molecules detected with this double-quantum filtering experiment. It is notable that a significant fraction of the ^{1}H NMR intensity is removed in the experiment, as only molecules with low local mobility, resulting in sustained dipolar couplings, can be observed.

Evidence for the participation of the flexible ethylene oxide and siloxane moieties in proton transport is provided in the ^{1}H NOESY NMR spectra of the materials. In contrast to the DQF spectra, the NOESY spectra acquired for mixing times above 2 ms under variable temperature conditions show strong correlations among all types of protons, consistent with weak couplings within a disordered, mobile material, as shown in Figure 4. What is clear from these spectra is that cross-peaks between all types of protons, including the N−H proton, are established for short mixing times. This is indicative of strong, incoherent interactions among the protons, as can be expected for a weakly coupled system. Thus the flexibility of the polymer architecture can be credited with providing the local mobility necessary for proton transport. Moreover, these data provide support for a Grotthus mechanism of proton-transport, in which H-bonding is retained (i.e., can be observed through the DQ filter), and yet dynamic, with bonds being broken and reformed as protons are passed along, as observed in the reduced DQF intensity. This process is supported by local mobility, including ring-reorientation, as evident from the exchange among aromatic and aliphatic ^{1}H resonances. These findings are consistent with the conductivity studies, in which Vogel−Tamman−Fulcher (VTF) fits were appropriate, rather than simple Arrhenius fits, due to the curved nature of the conductivity versus inverse temperature plots.[9,19] Such behavior is typically exhibited in conductors for which segmental motion plays an important role in the transport process.

Activation Energies Established via Variable-Temperature ^{1}H NMR. Single-pulse ^{1}H MAS experiments at variable temperature for the same samples are shown in Figure 5. Here, the temperature is varied in 10-degree steps between 310 and 350 K, with the sample temperature corrected to include the heating effects of spinning at 25 kHz.[20] This temperature range is above the glass transition temperatures of the materials (CImSS, $T_g = 296$ K; PImSS, $T_g = 314$ K), so significant local mobility is present. The temperature-dependent behavior of the N−H resonance, at 12 and 15 ppm for CImSS and PImSS, respectively, shows several trends. First, the line narrows with increasing temperature, and second, the chemical shift of the proton resonance in the N−H bond trends toward lower frequency with increasing temperature, with an overall shift difference of 1 ppm between 310 and 330 K for CImSS, and 4 pm between 310 and 350 K for PImSS. The gradual shift of the N−H resonance at higher temperature (Figure 5b) is interpreted as a coalescence process between hydrogen-bonded (high-frequency) protons, and a "free" proton resonance. This is contrasted with the Imi-2EO materials (Figure 5a), in which the first process is the coalescence

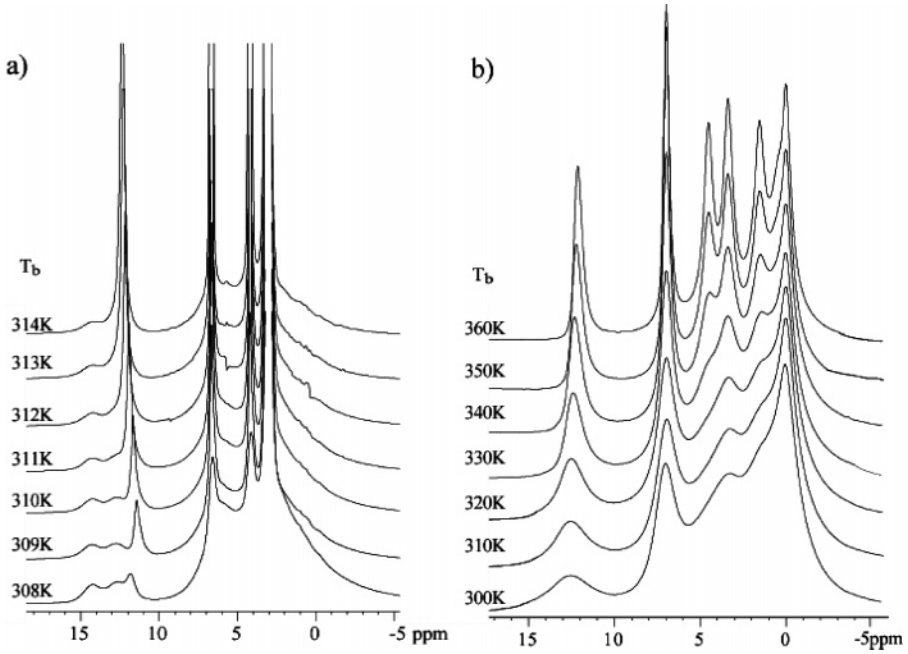

Figure 5. ^{1}H variable temperature MAS spectra of (a) Imi-2EO and (b) PImSS. Bearing gas temperatures (T_b) are noted on each spectrum.

between the different types of H-bonded domains, before a chemical shift trend to lower frequency, indicative of the increasingly dynamic H-bonding, is observed. The low-frequency, "free", proton resonance is not visible due to the overlap with the broad aromatic resonance; however it can be inferred due to the observed trends. This resonance would be expected approximately at a chemical shift of N−H in dilute solution, around 9 ppm. The chemical shift trend indicates a weak hydrogen-bonding network in the disordered, mobile phase as the samples soften. As was found for Imi-*n*EO, this dynamic hydrogen bonding is proposed to be the driving mechanism of proton transport, and is even more essential in these large molecules than in the smaller Imi-*n*EO materials, where $n = 1-5$. This chemical shift trend, together with the simultaneous filtering of both the aromatic and N−H resonances with the DQF sequence, illustrate the correlation between ring-reorientation and proton transport, which has been suggested for the Imi-*n*EO materials,[8] and discussed at length in a related salt, imidazolium methylsulfonate.[21]

The increasing mobility of the molecules is also reflected by the line width of the N−H resonance, which narrows in both systems with increasing temperature. Further examination of the N−H line width reveals a linear temperature dependence of the spin−spin relaxation time (T_2*) when plotted versus inverse temperature (Figure 6a). This relation allows us to obtain the activation energies (Table 1) for proton mobility in the systems of study. Results obtained from the above correlation for the triflic acid-doped materials are shown in Figure 6b.

The activation energies obtained (E_a (T_2*) = 47.4 ± 1.0 kJ/mol, CIm-SS; E_a (T_2*) = 44.8 ± 1.0 kJ/mol, PIm-Ss) for the new systems studied were comparable to those obtained by NMR for both Imi-*n*EO materials, and compare well, as listed in Table 1. Interesting contrasts are found by comparing the activation energies from conductivity measurements. These match relatively well for Imi-5EO (E_a (σ) = 52 ± 2.0 kJ/mol), but differ significantly for Imi-1EO (E_a (σ)= 128 ± 2.0 kJ/mol), which was highly ordered, and likely influenced by grain boundaries and limitations to proton transport in crystalline domains. We propose this local energy barrier found for PImSS and CImSS corresponds to the energy barrier for conductivity in samples where crystallinity and grain boundaries do not limit the macroscopic conductivity. We note that the two data sets are offset from each other along the temperature axis, corresponding to the ~20 degree difference in the T_g values of the two materials. The addition of acid dopant brings the glass transition tempera-

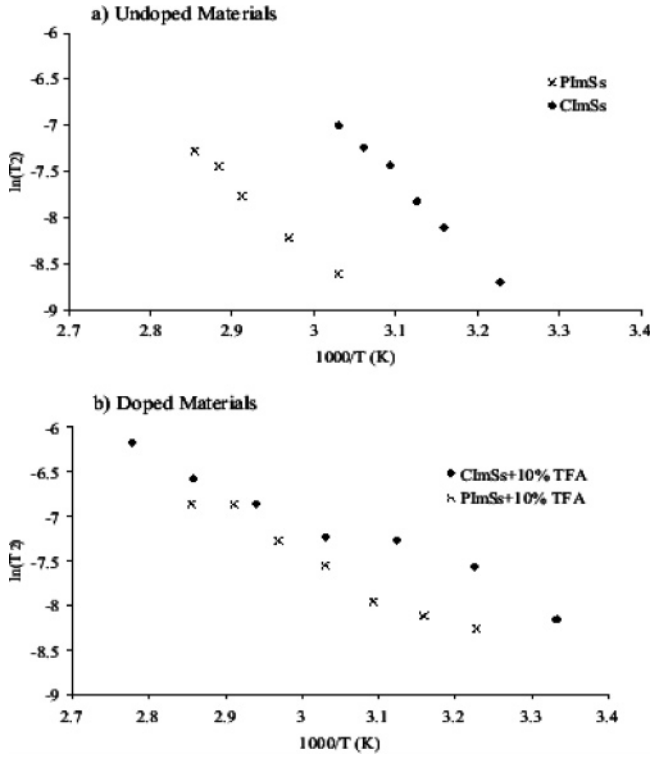

Figure 6. T_2 relaxation time versus 1000/T for (a) undoped and (b) triflic-acid-doped materials.

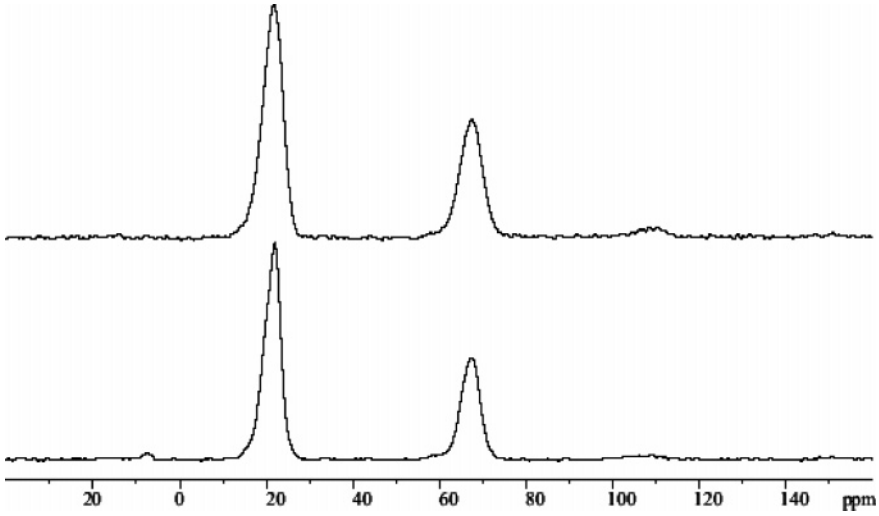

Figure 7. ^{29}Si CPMAS 2 kHz for PImSS (bottom) and CImSS (top).

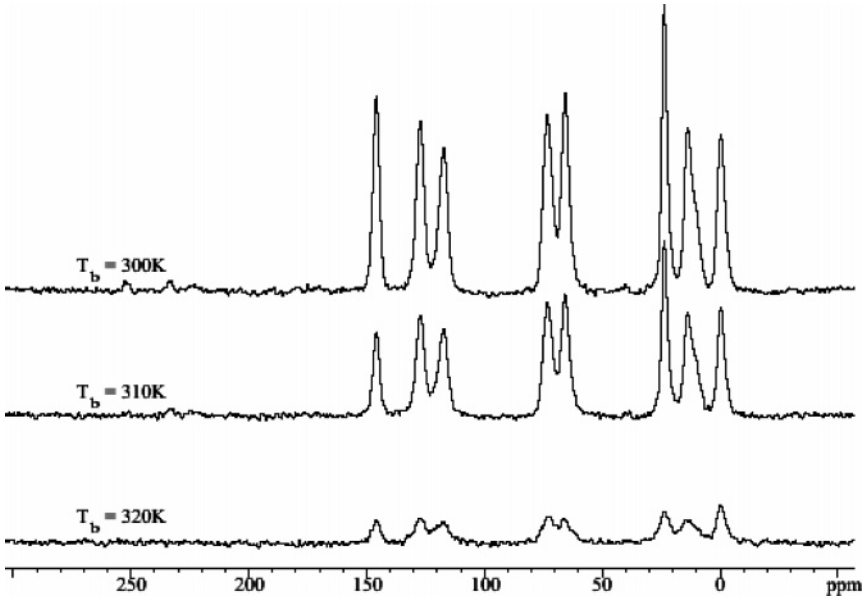

Figure 8. ^{1}H−^{13}C CPMAS on PImSS at 8 kHz MAS under variable temperature conditions.

Table 1. Activation Energy of Local Proton Mobility from ^{1}H NMR Line Width Data Compared to Conductivity Measurements

material	E_a (from conductivity) (σ) (kJ/mol)	E_a from NMR data (T_2*) (kJ/mol)
Imi-1EO[8]	128 ± 2	48 ± 1.0
Imi-5EO[8]	52 ± 2	60 ± 1.0
CImSS		47.4 ± 1.0
CImSS-doped		26.7 ± 1.0
PImSS		44.8 ± 1.0
PImSS-doped		23.5 ± 1.0

tures closer together, as observed in the overlapping trends in Figure 6b. Comparison between doped and undoped systems shows higher proton mobility in the doped systems as reflected by lowered activation energies calculated for the doped systems. This is consistent with the enhanced proton transfer by addition of an acid dopant, which simply increases proton concentration and facilitates the transfer via protonation/deprotonation of the imidazole N−H groups. The decreased T_g upon doping also contributes to enhancing local mobility, and thus decreasing the activation energy for transport. These results are in agreement with the conductivity measurements, which show an increase in proton conductivity upon addition of acid.[9]

To put these data in context, it is of interest to compare these activation energies for local proton mobility to those reported for Nafion, the industry benchmark in proton-conducting membranes.[4] The activation energy obtained from impedance spectroscopy measurements of conductivity is 9.34 kJ/mol,[22] and the activation energy obtained for local proton mobility is 8.64 kJ/mol.[23] The latter was measured using the same methods described in this paper. These values are notably smaller than those obtained for doped CImSS and PImSS, which is consistent with their comparably lower proton conductivities relative to Nafion. Nevertheless, in both cases we are able to identify the molecular-level process necessary to facilitate long-range proton transport.

Structure and Dynamics from Heteronuclear NMR Studies. Further structural information about the systems studied was obtained from ^{29}Si and ^{13}C MAS spectra,

(22) Costamagna, P.; Yang, C.; Bocarsly, A. B.; Srinivasan, S. *Electrochim. Acta* **2002**, *47*, 1023.
(23) Janzen, N. J.; Goward, G. R. unpublished data.

illustrated in Figures 7 and 8 , respectively. The ^{29}Si MAS spectra revealed the presence of an extra silicon resonance at a resonance around −65 ppm in addition to the expected resonance at 20 ppm. The resonance at 20 ppm is consistent with the expected silicon coordination of two Si−O bonds, and two Si−R bonds. The extra resonance, assigned to silicon with three Si−O bonds, and a single Si−R bond, indicates the presence of a partially cross-linked silicone network rather than a pure straight-chain polymer. ^{13}C spectra at variable temperatures indicate that upon temperature increase all molecules become mobile, reflected by a uniform decrease in peak intensity for all resonances, i.e., aliphatic and aromatic as the molecules become mobile and thus the cross-polarization efficiency is lowered. In contrast to this, one might have observed an initial coalescence of the aromatic ^{13}C resonances at 118 and 128 ppm, if the first motion were the 2-site ring-reorientation of the imidazole rings, followed by softening of the rest of the polymer chains. Again, this finding is consistent with the VTF model of conductivity, involving segmental motion and structural ion transport.

Conclusions

Overall, the results of this study clearly indicate the presence of a Grotthus mechanism for proton transport in the PImSS and CImSS materials. Support for this mechanism due to local segmental motion of the polymer chains is also demonstrated in both the NOESY spectra and the ^{1}H variable-temperature studies. Activation energies calculated from the line width trends of the N−H resonances are consistent with a nearly 2-fold decrease in activation energy upon addition of 15% triflic acid. This result agrees with earlier conductivity studies, in which a significant increase in conductivity was observed upon doping. The added acid is presumed to break up the hydrogen-bonding network, facilitating ring-reorientation, and thus structural, or Grotthus mechanism proton transport.

Acknowledgment. The authors are grateful Prof. Alex Bain for helpful discussions.

CM048301L